Development 125, 2053-2062 (1998)
Printed in Great Britain © The Company of Biologists Limited 1998
DEV5203

Drosophila EcR-B ecdysone receptor isoforms are required for larval molting and for neuron remodeling during metamorphosis

Margrit Schubiger[1], Andrew A. Wade[2], Ginger E. Carney[2], James W. Truman[1] and Michael Bender[2,*]

[1]Department of Zoology, University of Washington, Seattle, WA 98195, USA
[2]Department of Genetics, The University of Georgia, Athens, GA 30602, USA
*Author for correspondence (e-mail: bender@bscr.uga.edu)

Accepted 2 April; published on WWW 6 May 1998

SUMMARY

During the metamorphic reorganization of the insect central nervous system, the steroid hormone 20-hydroxyecdysone induces a wide spectrum of cellular responses including neuronal proliferation, maturation, cell death and the remodeling of larval neurons into their adult forms. In *Drosophila*, expression of specific ecdysone receptor (EcR) isoforms has been correlated with particular responses, suggesting that different EcR isoforms may govern distinct steroid-induced responses in these cells. We have used imprecise excision of a P element to create *EcR* deletion mutants that remove the *EcR-B* promoter and therefore should lack EcR-B1 and EcR-B2 expression but retain EcR-A expression. Most of these *EcR-B* mutant animals show defects in larval molting, arresting at the boundaries between the three larval stages, while a smaller percentage of *EcR-B* mutants survive into the early stages of metamorphosis.

Remodeling of larval neurons at metamorphosis begins with the pruning back of larval-specific dendrites and occurs as these cells are expressing high levels of EcR-B1 and little EcR-A. This pruning response is blocked in the *EcR-B* mutants despite the fact that adult-specific neurons, which normally express only EcR-A, can progress in their development. These observations support the hypothesis that different EcR isoforms control cell-type-specific responses during remodeling of the nervous system at metamorphosis.

Key words: *Drosophila*, Ecdysone receptor, Metamorphosis, Molting, Neuron remodeling

INTRODUCTION

In insects that undergo complete metamorphosis, steroid hormones (the ecdysteroids) act at the end of larval life to transform the larva into an adult. During this dramatic transformation, ecdysteroids induce the differentiation of adult structures from imaginal precursor cells and induce most larval tissues to undergo programmed cell death. Cellular ecdysteroid responses during metamorphosis are particularly well documented in the central nervous system (CNS) of the moth *Manduca sexta* due to the large size of individual neurons and the feasibility of ligation experiments, which deprive developing cells of hormone, and hormone replacement experiments. Thus, ecdysteroids have been shown to control proliferation, maturation, or cell death of various neurons in the *Manduca* CNS during metamorphosis (reviewed by Truman, 1996). An interesting difference between the CNS and other tissues during metamorphosis is that significant numbers of larval neurons are remodeled and persist into the adult so that the adult CNS is a mosaic of larval and imaginal neurons. This remodeling process, initiated by the pruning back of larval dendrites and axonal arbors and followed by regrowth and formation of adult-specific synapses, has also been shown to be under ecdysteroid control (Weeks and Truman, 1985; Weeks, 1987; Levine and Weeks, 1996).

Although neuronal ecdysteroid responses during metamorphosis are best characterized in *Manduca*, *Drosophila* offers the opportunity to analyze these responses using molecular genetic approaches. Immunostaining in *Drosophila* has been used to mark small sets of neurons and follow them through development. These studies show that, as in *Manduca*, many larval *Drosophila* neurons persist through metamorphosis into the adult stage (reviewed by Truman, 1990; Truman et al., 1993). One well-characterized example of neuronal remodeling takes place in a set of neurosecretory cells that react with an antibody directed against the small cardioactive peptide (SCP) B (Truman, 1990).

In *Drosophila*, the response of tissues to ecdysteroids is mediated by a heterodimer of the EcR and USP proteins (Koelle et al., 1991; Koelle, 1992; Yao et al., 1992; Thomas et al., 1993; Yao et al., 1993), both nuclear receptor proteins. The *EcR* gene encodes 3 isoforms, EcR-A, EcR-B1 and EcR-B2, which share common DNA- and ligand-binding domains but differ in their N-terminal sequences. Tissues that have similar responses to ecdysteroids at metamorphosis have been shown to express similar EcR isoforms. Thus, imaginal discs express high levels of EcR-A and low levels of EcR-B1 at the time of puparium formation, while most larval tissues, as well as the imaginal histoblasts of the midgut islands and abdominal nests, express predominantly EcR-B1 at this time (Talbot et al., 1993).

The most extensive analysis of EcR expression has been performed on the CNS, and encompasses the period from larval hatching to adult eclosion (Truman et al., 1994). This analysis revealed a complex temporal and spatial pattern of EcR-A and EcR-B1 isoform expression through metamorphosis (EcR-B2 expression has not been determined because no antibody currently exists that recognizes the 17 amino acid EcR-B2 specific domain). The expression of the two isoforms early in metamorphosis correlates with the ongoing developmental responses, and not with the developmental origin of the cells, i.e. whether they are larval or imaginal neurons. Thus, EcR-B1 is expressed predominantly in neurons undergoing regressive responses whereas EcR-A is predominant in neurons showing maturational responses. Although correlative in nature, these observations are consistent with the hypothesis that EcR-A and EcR-B1 trigger specific cellular responses during CNS metamorphosis (Truman et al., 1994).

The recent isolation of *EcR-B1* specific mutations has allowed tests of EcR-B1 functions in directing specific responses to ecdysteroids (Bender et al., 1997). In contrast to mutations in *EcR* common exons, which inactivate all EcR isoforms and lead to embryonic lethality, mutations in an *EcR-B1* specific exon result in larval viability, but lethality at the onset of metamorphosis. As expected, *EcR-B1* mutations cause defects in larval and imaginal tissues that normally express high levels of EcR-B1, but do not obviously affect the differentiation of the imaginal cells that are predominantly EcR-A expressing. As a consequence, at the start of metamorphosis some developmental processes proceed, whereas others are arrested and development becomes desynchronized.

We have extended our analysis of EcR functions by isolating deletion mutations that remove the *EcR-B* transcription start site and therefore should lack both EcR-B1 and EcR-B2 and examining the effect of loss of EcR-B functions on the remodeling of larval neurons. Loss of both EcR-B isoforms leads to death predominantly at the first and second larval molt. Some *EcR-B* mutant larvae survive to the third larval instar, allowing investigation of EcR-B isoform function during metamorphosis of the CNS. Our results show that early pruning back of larval-specific processes in a defined set of larval neurons fails to take place in the *EcR-B* mutants, even though other aspects of CNS development progress. Mutations affecting only EcR-B1 do not lead to this block, suggesting that both EcR-B isoforms may be required for the loss of larval identity in these neurons.

MATERIALS AND METHODS

Imprecise excision screens

The insertion site of the PW45-4 P element was determined by sequencing an inverse PCR product (Sambrook et al., 1989) containing the 5′ junction between the P element and flanking genomic sequences. PCR primer sequences used were as described by Yeo et al. (1995).

Candidate *EcR-B* deletions were isolated in two screens by mobilizing the PW45-4 P element insertion using the transposase source P[Δ2-3] (Robertson et al., 1988). In one screen, 108 independent *white* derivative strains were established from the progeny of separate cultures of four pairs of *w; EcR^{PW45-4}/CyO; Δ2-3 Sb* females crossed to *w; Sco/SM6b* males. Because the EcR^{PW45-4} chromosome fails to complement *EcR* mutants, precise excisions were eliminated by discarding those derivative lines that complemented an *EcR* null allele, EcR^{M554fs} (Bender et al., 1997). Of the remaining 59 strains, seven strains lacked the 5′ and 3′ junction fragments between the P element and flanking genomic sequences as determined by PCR. The sequence of the 5′ junction fragment primers are, 5′-CGATGATGGCACTCATACTC-3′ (–322 to –343 nucleotides (nt) relative to the EcR-B1 transcription start site) and 5′-TCCAGTCACAGCTTTGCAGC-3′ (nt 172 to 191 within the P element; O'Hare and Rubin, 1983) resulting in a 480 nt product from the PW45-4 strain. The sequence of the 3′ junction fragment primers are, 5′-CACTCGCACTTATTGCAAGC-3′ (nt 2833-2852 within the P element) and 5′-ATTGGATTCCAAGGTGCCCC-3′ (nt +790 to +809 relative to the *EcR-B1* transcription start site) resulting in a 1022 nt fragment from the PW45-4 strain. The first and last of the primers listed above generate a 1243 nt PCR product from the wild type and allow assessment of whether derivatives retain short P element sequences near the PW45-4 insertion site. Five of the remaining seven lines showed no evidence of such footprints and were retained for Southern analysis. In a second screen, 80 independent *white* derivative strains were established from the progeny of individual *yw; EcR^{PW45-4}/CyO; Δ2-3 Sb* males crossed to *yw; Sco/CyO,y^+* females. Precise excisions were eliminated by complementation crosses to an *EcR-B1* mutant, EcR^{W53st} (Bender et al., 1997). Of the remaining 29 lines, four were tested by the PCR assays described above and three lack both 5′ and 3′ junction fragments and show no evidence of footprints.

Southern analysis and sequence determination of B1/B2 deletions

Southern blots of genomic DNA from the eight derivative strains lacking both 5′ and 3′ junction fragments were probed with a 1.7 kb *Eco*RI cDNA fragment containing exon 1 and exon 2 sequences or one of three contiguous genomic *Eco*RI fragments (Fig. 2) located between –3 kb and +6 kb of the EcR genomic walk (Koelle et al., 1991). Six strains contained deletions of less than 3.5 kb. To refine the deletion endpoints for these strains, primers flanking exon 1 were used to PCR amplify deletion fusion fragments. Deletion fusion fragments were successfully amplified for EcR^{2}, EcR^{214}, EcR^{225}, EcR^{80} and EcR^{99} using one of three upstream primers (located between 1 and 3 kb upstream of exon 1) and one of three downstream primers (located between 1 and 3 kb downstream of exon 1).

Western analysis

Protein samples for wild-type Canton-S controls were prepared from 10 white pre-pupae. Protein samples for the homozygous *EcR-B* mutant lines were made from 5-10 mutant animals that had emptied their guts, and had become very sluggish or stopped moving. Based on these externally visible criteria and also on the extent of disc eversion in such animals (data not shown), this stage is comparable to a control animal at the white puparium stage. Animals were homogenized in 2× sample buffer (125 mM Tris, 4% SDS, 20% glycerol, 0.005% bromophenol blue, 10% β-2-mercaptoethanol), boiled for 3 minutes and centrifuged at 10,000 ***g*** at 4°C. The supernatant was boiled again for 3 minutes, and equilibrated to room temperature before loading. Protein from the equivalent of one animal was loaded in each lane on an 8% acrylamide SDS gel. Protein was transferred to nitrocellulose filter, blocked with 5% dry milk and 5% BSA in TBS (Tris-buffered saline, pH 7.8) + 0.1% Tween-20 for 1 hour. The blots were incubated in monoclonal antibody directed against EcR-B1 (AD4.4) or EcR-A (15G1A) (Talbot et al., 1993) at a 1:50 dilution for 1 hour at room temperature and then rinsed in TBS-Tween 5× over the course of 1 hour. A peroxidase coupled goat anti-mouse secondary antibody (Jackson Lab) was used at 1:1000 dilution (1 hour at room temperature) and rinsed as before. EcR was detected with the ECL kit (Amersham) according to manufacturer's instructions. The blots were stripped according to manufacturer's

instructions and reprobed. After transfer of the gel to nitrocellulose filter, the gel was stained with Coomassie blue (Sambrook et al., 1989). The non-transferred high molecular weight proteins were used as loading controls.

Lethal phase determination

EcR-B mutant animals were marked with *yellow* (*y*) using the second chromosome balancer CyO,y^+. Six-hour egg collections were made on grape juice agar plates 2-4 days following the mating of 25 *yw; EcR-B/CyO,*y^+ males to 25 *yw;* $EcR^{M554fs}/CyO,y^+$ virgin females. The sample size was greater than 200 eggs per genotype. At 36 hours after the end of the egg collection period, plates were scored for living *y* and y^+ first instar larvae. Since homozygous CyO,y^+ individuals die during embryogenesis, the number of *y* mutant larvae should be half the number of y^+ if there is no mortality. The number of *y* mutant larvae (*yw; EcR-B/*EcR^{M554fs}) was divided by one half the number of y^+ sibling larvae (*yw; EcR-B/CyO,*y^+ and *yw;* $EcR^{M554fs}/CyO,y^+$) to obtain the percentage survival for each genotype shown in Table 1. As necessary, *y* larvae were transferred to fresh plates and scored again at 60 hours, 96 hours, and 168 hours after egg deposition for second instar, third instar, and pupal *y* animals.

Immunocytochemistry

Central nervous systems were dissected in PBS and fixed for 1-2 hour in 4% formaldehyde. After several rinses with 0.3% Triton X-100 in PBS (PBS-Tx) the tissue was blocked for 15-60 minutes in 5% normal goat serum in PBS-Tx. Incubation of the tissue in primary and secondary antibodies was done overnight at 4ºC in PBS-Tx + 1% normal goat serum. The primary antibodies were used at 1:50 for anti-EcR-B1 (AD4.4) and anti-EcR-A (15G1A), at 1:400 for anti-SCP (Masinovsky et al., 1988), and 1:500 for anti-chaoptin (Zipursky et al., 1984; a gift from H. Steller). FITC- and Texas Red-conjugated secondary antibodies (Jackson Lab) were diluted 1:1000. The tissue was rinsed, dehydrated and embedded in DPX (Fluka) and analyzed with a Bio-Rad MRC 600 confocal microscope. For the SCP labeled preparations we took z-series at 1.4 μm intervals through the CNS and projected the images.

RESULTS

Isolation of *EcR-B* deletions by imprecise excision of a P-lacW transposon insertion

The EcR-B1 and EcR-B2 proteins are produced from alternatively spliced messenger RNAs from the *EcR-B* promoter (Fig. 1) that lies approximately 35 kilobases (kb) downstream from the *EcR-A* promoter (Talbot et al., 1993). The P element insertion mutation *PW45-4*, isolated in a 2nd chromosome insertional mutagenesis (Torok et al., 1993), is an *EcR* allele as it fails to complement *EcR* null mutations (data not shown). The insertion point of this element maps to a position 32 nucleotides (nt) upstream of the *EcR-B* transcription start site (Fig. 1, see Materials and Methods). Because EcR-B1 protein is detected on western blots prepared from EcR^{PW45-4} homozygotes (data not shown), the insertion does not completely inactivate EcR-B isoform function.

To completely eliminate EcR-B isoform expression, we isolated small *EcR* deletion mutations by scoring for loss of the *mini-white* marker gene contained within the PW45-4 element (Bier et al., 1989) following mobilization of the element by the P[Δ2-3] transposase source (Robertson et al., 1988). Of 188 independent *white* derivatives, 100 were eliminated genetically as precise excisions (see Materials and Methods) leaving 88 candidate imprecise excision lines. PCR analysis showed that eight of these lacked both 5′ and 3′ junction fragments between the P element and flanking genomic sequences, suggesting a deletion of the entire P element. Of these 8 strains, 6 (EcR^2, EcR^{214} EcR^{225}, EcR^{31}, EcR^{80} and $EcR^{99)}$ were shown to be limited to 3.5 kb or less in size by Southern blot and PCR analysis. Three of these lines (EcR^2, EcR^{214} and EcR^{225}) lack the *EcR-B* transcription start site while the remaining three (EcR^{31}, EcR^{80} and EcR^{99}) lack either the start site or sequences immediately upstream of the start site (Fig. 2).

In extracts from mutants homozygous for EcR^{31}, EcR^{80}, EcR^{99}, EcR^{214}, or EcR^{225}, EcR-B1 protein is not detected, while EcR-A protein is present (Fig. 3). In comparison, a wild-type control at a comparable stage produces both EcR-B1 and EcR-A protein (Fig. 3). EcR^2 mutant homozygotes were not tested because these animals do not survive to this stage. Thus, all *EcR-B* deletion strains tested lack EcR-B1 protein but produce EcR-A protein. Since EcR-B2 and EcR-B1 are produced from the same primary transcript, we presume that the *EcR-B* mutants are inactive for EcR-B2 as well as EcR-B1.

EcR-B mutants exhibit defects in larval molting

The percentage of mutants surviving at different developmental stages when heterozygous for an *EcR-B* allele and the null allele EcR^{M554fs} is shown in Table 1. The majority of mutant animals

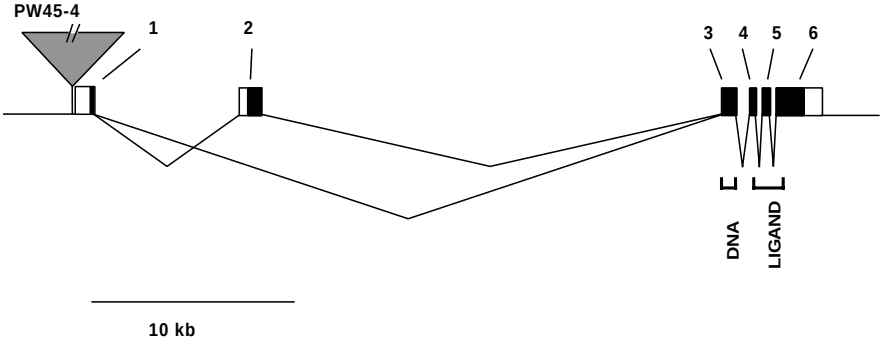

Fig. 1. Location of a P element insertion near the *EcR-B* transcription start site. The insertion site of the PW45-4 P element (at nucleotide −32) is shown relative to the *EcR-B* transcription start site. The *EcR-B1* mRNA (including exons 1 through 6) and the *EcR-B2* mRNA (including exons 1 and 3 through 6) are produced by alternative splicing of a transcript from the *EcR-B* promoter. Protein coding sequences are indicated by black boxes and sequences encoding DNA and ligand binding domains are bracketed. The amino terminus of EcR-B2 (17 residues) is encoded by exon 1, while the amino terminus of EcR-B1 (226 residues) is encoded by exon 2. The EcR-B1 open reading frame does not begin at the EcR-B2 AUG because of stop codons in the upstream portion of exon 2. The *EcR-A* promoter lies approximately 35 kb upstream of the *EcR-B* promoter shown here. The EcR-A protein is produced from an mRNA consisting of three upstream EcR-A specific exons and exons 3 through 6. The *EcR* gene structure was described by Talbot et al. (1993).

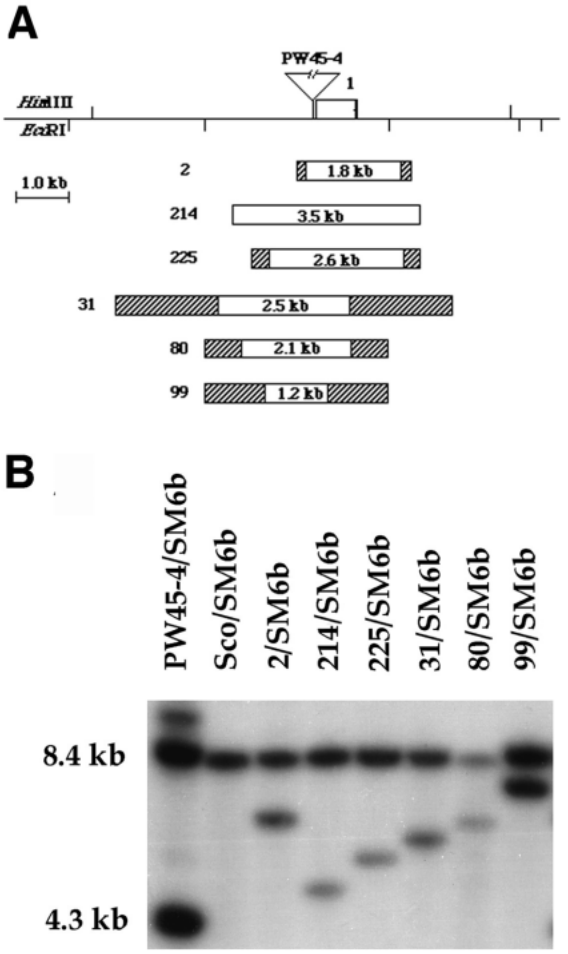

Fig. 2. Deletions that remove the *EcR-B* transcription start site. (A) The genomic region that includes exon 1 is shown at the top. *Hin*dIII sites are indicated above the line and *Eco*RI sites below the line. The extents of deletions generated by imprecise excision of the PW45-4 transposon are indicated by white bars. Hatched regions indicate the current uncertainty in the position of the deletion endpoints. (B) A Southern blot of genomic DNA from *EcR-B* deletion strains digested with *Hin*dIII and hybridized with a probe prepared from the 3.5 kb *Eco*RI fragment that includes exon 1. Reductions in size of between 1.2 and 3.5 kb are seen in the 8.4 kb *Hin*dIII genomic fragment. The 4.3 kb doublet seen in the PW45-4 parental lane is due to the 5′ and 3′ junction fragments between P element and genomic sequences. The 10 kb fragment in this lane is due to hybridization of plasmid sequences from the probe to plasmid sequences contained within the P-lacW element. DNA from *w; Sco/SM6b* flies (lane 2) is included as a wild type control for the *Hin*dIII fragment size.

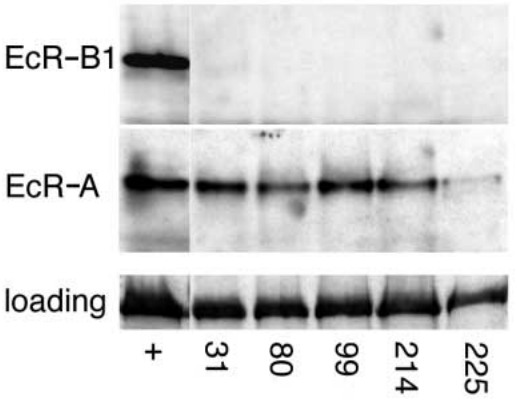

Fig. 3. Expression of EcR-A and EcR-B1 in *EcR-B* mutant strains. Extracts from animals homozygous for a given *EcR-B* deletion were assayed by western blot for the presence of EcR-A and EcR-B1 protein isolated from whole animal preparations. Western filters were probed with the EcR-B1 specific antibody AD4.4 (top panel) or the EcR-A specific antibody 15G1A (center panel). The extract in the first lane (+) is from wild-type Canton-S animals at the white prepupa stage. Extracts were made from homozygous *EcR-B* deletion strains at a comparable developmental stage. A high molecular weight band of a Coomassie stained gel after transfer (bottom panel) is shown to indicate protein loading.

Table 1. *EcR-B* lethal phase

	Stage			
Allele	1st larval	2nd larval	3rd larval	pupal
2	95 (36)	8	0	–
214	106 (37)	14	3	0
225	110 (48)	23	9	0
80	108 (83)	31	5	0
99	97 (44)	42	2	0
31	102 (27)	60	23	0
M554fs	0 (0)	–	–	–
W53St	123 (50)	114	47	0

EcR-B mutants heterozygous for the null allele EcR^{M554fs}, recognizable by the *y* marker, were scored for survival at four times during development. The values shown are percentages of *y* animals expected from the number of *y+* 1st instar sibling larvae obtained from each cross and therefore sometimes exceed 100% (see Materials and Methods). The number of *y* 1st instar larvae is shown in parentheses. Percent survival of the common exon mutant EcR^{M554fs} and the *EcR-B1* mutant EcR^{W53st} are shown below the dotted line for comparison. These values are comparable to those previously obtained for *EcR* common region and *EcR-B1* specific mutants (Bender et al., 1997).

fails to survive to the 2nd larval instar and few mutant animals survive to the 3rd larval stage. Thus, the predominant time of death of *EcR-B* mutants is during the 1st and 2nd larval stages.

The *EcR-B* lethal period can be contrasted with the strong embryonic lethality of *EcR* common exon mutations (e.g. EcR^{M554fs}; Bender et al., 1997) that inactivate all three EcR isoforms (Table 1, bottom). The *EcR-B* lethal period also differs from that seen for the *EcR-B1* specific stop codon mutant, EcR^{W53st} (Bender et al., 1997), in that the *EcR-B1* mutant shows little reduction in 2nd larval stage viability and has substantially greater numbers of surviving 3rd instar larvae than any of the *EcR-B* mutants (Table 1, bottom). Thus the *EcR-B* lethal phase differs from that of both *EcR* null and *EcR-B1* specific mutants.

The *EcR-B* animals that arrest during larval development showed defects in the process of larval molting. Animals arrested prior to the 2nd larval stage carry both 1st and 2nd larval mouth hooks (Fig. 4A) while those arrested prior to the 3rd larval stage carry both 2nd and 3rd larval mouth hooks (Fig. 4B). For the genotypes tested (EcR^{31}/EcR^{M554fs}, EcR^{80}/EcR^{M554fs}, and EcR^{99}/EcR^{M554fs}) 65-80% of the larvae examined showed this phenotype. These animals also appear to retain the cuticle from the previous instar in addition to their

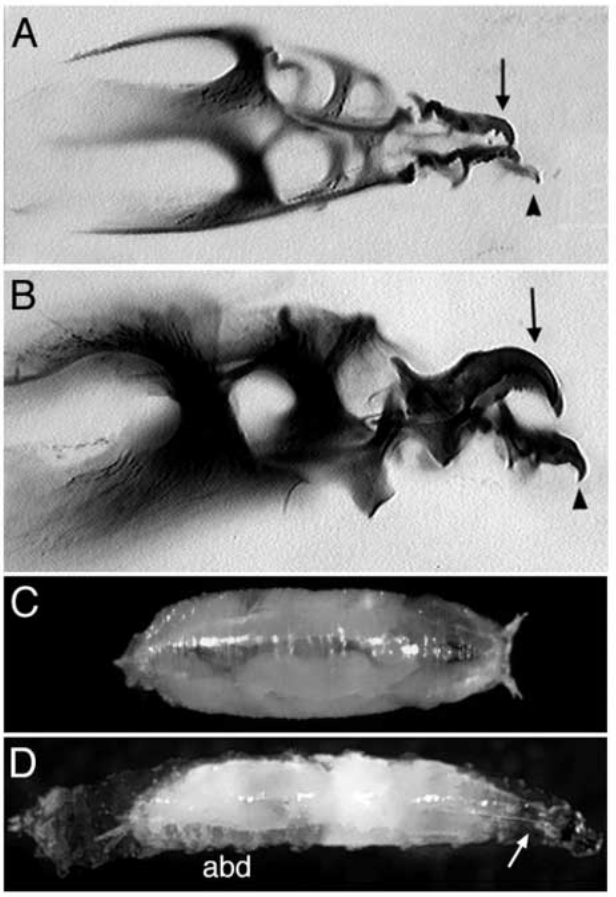

Fig. 4. Phenotypes of *EcR-B* mutants defective in larval molting (A,B) and pupariation (C,D). (A) EcR^{214} homozygous animal arrested during the first larval instar. First and 2nd instar mouth hooks are indicated by the arrowhead and arrow, respectively. (B) EcR^{214} homozygous animal arrested during the 2nd larval instar with both the 2nd (arrowhead) and 3rd (arrow) instar mouth hooks. (C) Control EcR^{214}/CyO,y^+ white prepupa. (D) An EcR^{214} homozygous non-pupariating animal, with abdominal (abd) segments visible. Arrow indicates detached mouth hook and anterior retraction of the animal fom the larval cuticle.

newly formed cuticle (data not shown). Therefore, the majority of the mutants arrest during the process of molting.

Phenotype of late arrested EcR-B mutants

A small fraction of the *EcR-B* mutants survive to the third larval stage (Table 1). These animals feed and later come to the surface of the food, but do not wander up the sides of the vial, indicating that normal wandering behavior is affected. They then become sluggish and eventually immobile. Wild-type larvae empty their gut at the end of the wandering period, shortly before the animals contract and form the barrel-shaped puparium. The mutant animals empty their gut but do not contract or form a tanned puparium. In addition, the gas bubble that normally forms at about 3 hours after pupariation is not observed in *EcR-B* mutants. Nevertheless, some tissues in these arrested larvae continue to show developmental changes: the larval cuticle apolyzes and a large space between the cuticle and the epidermis appears at the anterior and posterior ends (Fig. 4D), although the tracheal trunks remain attached to the larval cuticle. Later, the mouth hooks are expelled, a process that normally occurs at 12 hours after pupariation, at the time of head eversion. It is evident that a new cuticle, presumably the pupal cuticle, has been secreted (see for example Fig. 5B, showing autofluorescence of the cuticle secreted by the eye-antenna disc) and demarcation of the abdominal segments can be distinguished (Fig. 4D).

Elongation of the imaginal discs in mutant animals begins normally up to a stage comparable to about 4 hours after pupariation. At this time the peripodial epithelium contracts in wild-type animals to allow the discs to evert to the exterior (Fristrom and Fristrom, 1993). In the mutants this contraction apparently does not occur and the uneverted discs continue to elongate, but within vesicles inside of the body (data not shown). The appendage can then break through the peripodial membrane and elongate inside the body.

In normal development the beginning of muscle histolysis is recognizable at 3 hours after pupariation by a loss of birefringence in the set of larval abdominal muscles that are histolyzed during the prepupal stage (Kimura, 1990). In the mutants even at the time of mouth hook detachment the larval muscles are present and have retained their birefringence. In the gut, the larval gastric cecae which normally histolyze during the prepupal stage (Jiang et al., 1997) have shortened but are still present at the time of the developmental arrest (data not shown).

In wild-type animals the CNS undergoes drastic morphological changes between the time of pupariation and head eversion (Fig. 5C). The ventral nerve cord elongates, the subesophageal ganglion begins to separate from the thoracic ganglia and the optic lobes expand. These changes also occur in the late stage arrested mutants and can be extensive (compare Fig. 5A and B). On a cellular level, advancement of development can be seen in the attainment of chaoptin-immunoreactivity in interneurons of the optic lobes. At the onset of metamorphosis (Fig. 5D) chaoptin is expressed in the photoreceptors that project into the lamina and medulla (Zipursky et al., 1984), but not in optic lobe interneurons. As development progresses a set of medullar interneurons (Fig. 5F) begin to express the chaoptin antigen. In the mutants we see the same progression with interneurons clearly labelled in the late arrested animals (Fig. 5E).

In summary, in the *EcR-B* mutants some processes reach the stage of the prepupal/pupal transition (i.e. pupal cuticle secretion and morphological changes in the CNS), whereas other processes do not occur (contraction and tanning of the larval cuticle to form the puparium, muscle and midgut histolysis).

Effects of *EcR-B* mutations on remodeling of larval neurons

EcR-A and EcR-B1 expression levels have been characterized for different neurons and glia cell types throughout metamorphosis (Truman et al., 1994). Many of the developmental changes in these cells can be correlated with particular EcR expression patterns. Here we focus on larval neurons that undergo remodeling to change from their larval form to that of an adult. At the onset of metamorphosis they lose their synaptic targets and begin to prune back their larval dendritic and axonal arbors. This first step in the remodeling

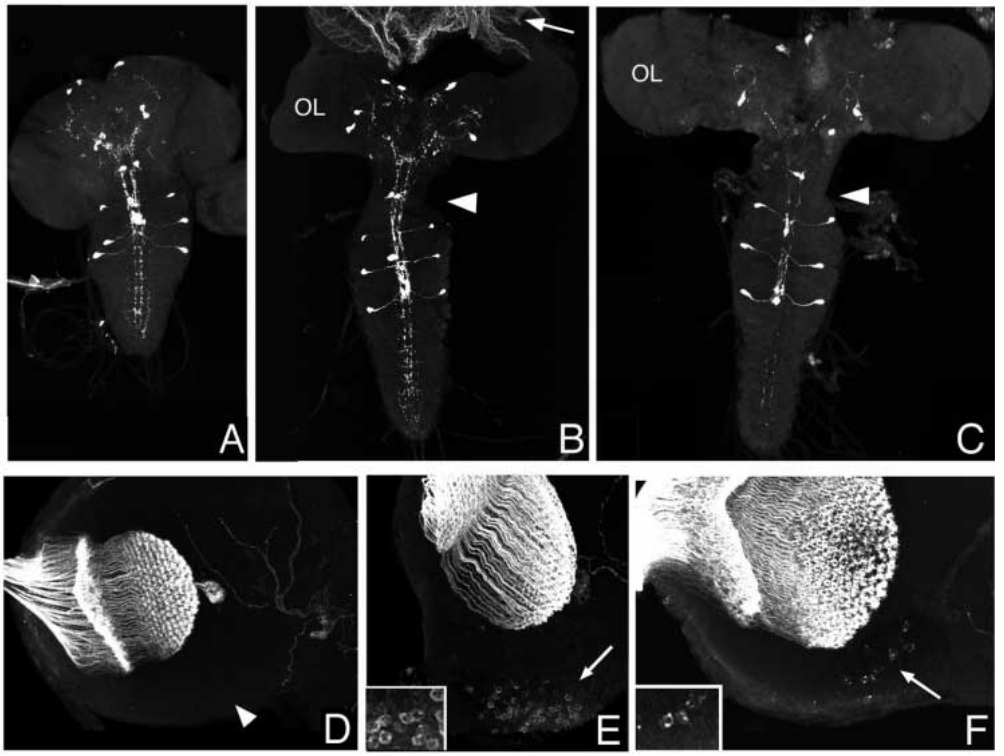

Fig. 5. Morphogenetic changes in the CNS of *EcR-B* mutants. (A-C) Low magnification confocal images of the CNS from an EcR^{99} homozygous mutant at late wandering stage (A), and at the time of developmental arrest (B). The CNS has elongated, the subesophageal ganglion has begun to separate from the ventral nerve chord (arrowhead) and the optic lobes (OL) have expanded. Note the autofluorescence of the pupal cuticle secreted by the eye-antennal disc (arrow). (C) CNS from a control animal ($EcR^{99}/CyO,y^{+}$) at the time of head eversion. Arrowhead, separation of the subesophageal ganglion from the thoracic neuromeres; OL, expanded optic lobes. CNS preparations were immunostained using the SCP antibody. (D-F) Chaoptin-immunoreactivity in the optic lobes. (D) Control ($EcR^{214}/CyO,y^{+}$) at white puparium stage. The projecting photoreceptors are strongly immunoreactive, but no interneurons (arrowhead) are labeled. (E) Late stage arrested homozygous EcR^{214} animal with chaoptin-expressing interneurons (arrow and higher magnification insert). (F) Control animal at head eversion with immunopositive interneurons (arrow and insert).

process is preceded by high levels of EcR-B1 expression. Later during pupal development EcR-A is the predominant isoform expressed in these neurons and it is during this stage that adult-specific processes and synapses are made. From the correlation of the EcR expression patterns with the ongoing developmental changes, Truman et al. (1994) suggested a functional role for the two EcR isoforms. Process regression for example would be under the control of EcR-B1, whereas maturation would be induced by EcR-A. Since there are no antibodies available against EcR-B2, such a correlation cannot be made so far for this isoform.

The null mutations for the EcR-B isoforms allow us to test for a functional role of EcR isoform types. We focused on a small set of larval neurons that contain a peptide that cross-reacts with an antibody against the molluscan small cardio-active peptide B (SCP) (Truman, 1990). These neurons are a subset of the FMRFamide expressing neurons (Schneider et al., 1993). The SCP antibody strongly labels the neurons and reveals a characteristic projection pattern that can easily be followed as these larval neurons initiate remodeling.

Fig. 6A shows the EcR-B1 expression of SCP labeled neurons in control white puparia, and demonstrates that these

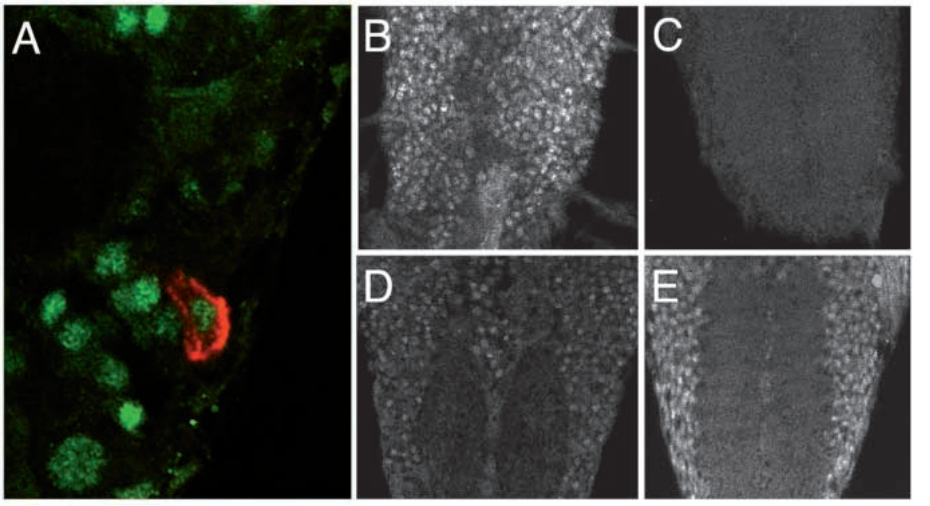

Fig. 6. EcR expression in SCP-immunoreactive cells. (A) EcR-B1 (green) and SCP (red) double labeling in the ventral nerve cord of a 0 hours AP control animal ($EcR^{PW45\text{-}4}/CyO,y^{+}$). The SCP labeled neuron is one of the ventral thoracic cells of a prominent pair of neurons (Tvs) in each thoracic segment (see Fig. 7). (B,C) EcR-B1 expression in ventral nerve cords from a 0 hours AP control ($EcR^{214}/CyO,y^{+}$) (B) and an *EcR-B* excision line (EcR^{214}/EcR^{214}) (C). In the homozygous *EcR-B* excision line EcR-B1 is not detected above background. (D,E) EcR-A expression in neurons in 0 hours AP CNSs from control ($EcR^{80}/CyO,y^{+}$) (D) and mutant (EcR^{80}/EcR^{80}) (E) animals. EcR-A is detected in both genotypes.

neurons, as well as many surrounding larval neurons, express EcR-B1 at the time of pupariation. The *EcR-B* mutants show no detectable EcR-B1 immunoreactivity (compare Fig. 6B and C), as expected from the western data (Fig. 3), whereas the neurons of controls and mutants at the same stage both express EcR-A (Fig. 6D and E).

The SCP labeling pattern in the ventral nerve cord of control 0 hour prepupa (Fig. 7A) is distinguished by a prominent pair of ventral neurons in each thoracic neuromere (the Tv neurons; Schneider et al., 1993) and several other neurons in the subesophageal ganglion (White et al., 1986; Lundquist and Nassel, 1990; Taghert and Schneider, 1990). The neurites from these cells form a characteristic projection pattern that is particularly dense in the area of the subesophageal ganglion, forming a posteriorly directed branch. Shortly after pupariation the dendritic arbors begin to regress (Truman, 1990). By 5-6 hours after pupariation (Fig. 7B) the SCP label is clearly reduced, and at the time of head eversion (Fig. 7C) few dendrites remain.

As previously discussed (Truman, 1990), we attribute the loss of labeled dendrites to be caused by the regression of the dendritic arbors, rather than the loss of the neuropeptide from the finer processes. To test this interpretation we have expressed the bovine microtubule-associated protein tau in a subset of the SCP-IR neurons. Using the GAL4-UAS system (Brand and Perrimon, 1993) we have made GAL4 constructs with upstream sequences of the FMRFamide gene (Schneider et al., 1993) to drive UAS-tau (Ito et al., 1997) in the Tv cells. Examination of the Tau pattern at pupariation and late prepupal stages revealed a clear reduction of processes in the older animals (S. Robinow, M. S. and J. W. T., data not shown). This indicates that the reduced SCP labeling pattern we see as

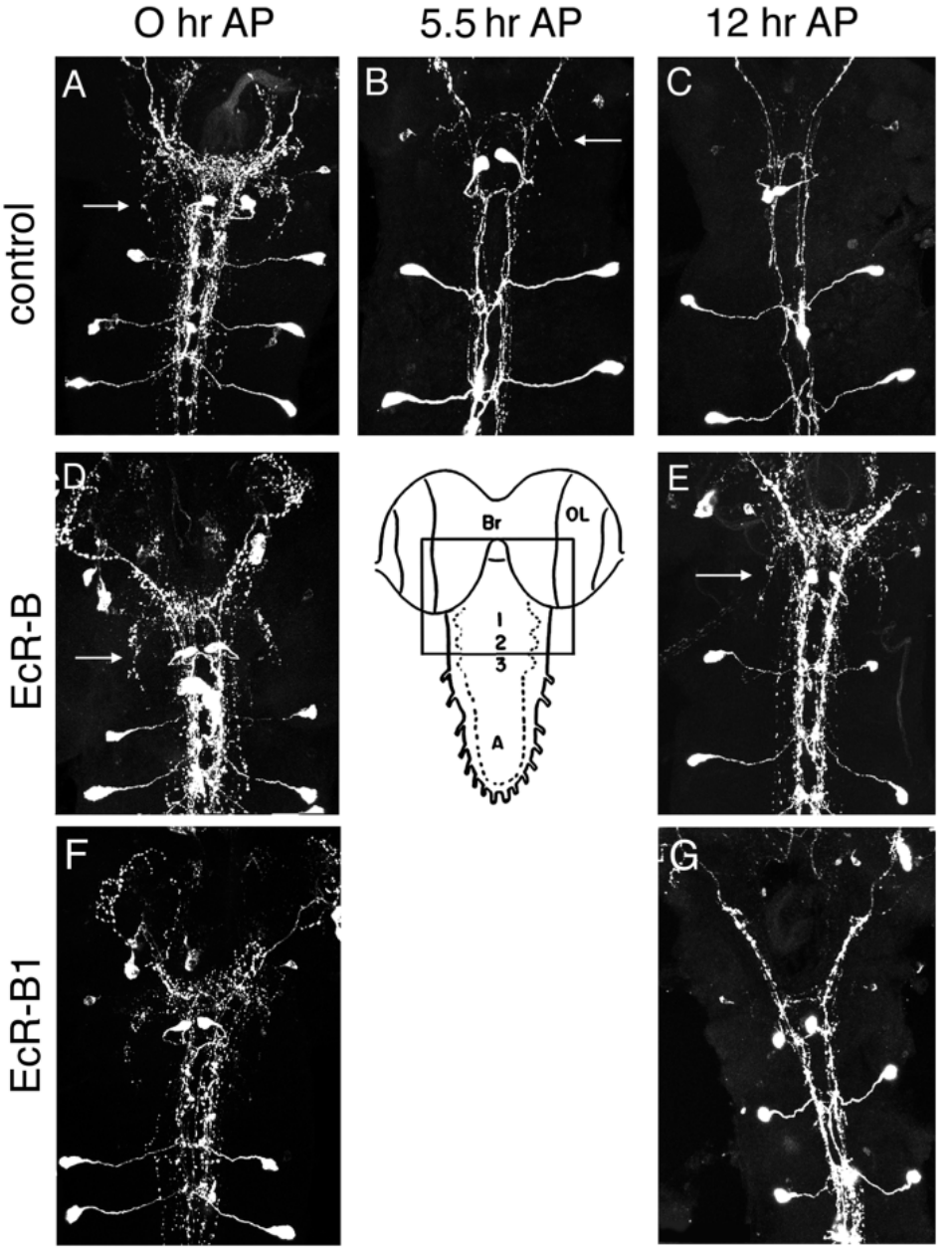

Fig. 7. SCP immunostaining in control ($EcR^{99}/CyO,y^{+}$) (A-C), *EcR-B* excision line (EcR^{99}/EcR^{M554fs}) (D-E), and *EcR-B1* specific mutant (EcR^{Q50st}/EcR^{M554fs}) (F-G) CNS. Box in the diagram indicates area of the micrographs. All panels are projections of confocal z-series. (A) SCP staining pattern at 0 hours AP forming dense dendritic arbors with a characteristic posteriorly directed branch (arrow) in the area of the subesophageal ganglion. A prominent pair of neurons (Tvs) in each thoracic neuromere, as well as few cell bodies anteriorly are labeled. (B) Control CNS 5.5 hours AP. The cell bodies are strongly labeled but the arbor (arrow) is reduced. (C) Control CNS 12 hours AP. Reduction of the dendritic arbor is extensive and only a few processes are visible. The cell bodies remain strongly immunoreactive. (D) SCP staining pattern in the CNS of an *EcR-B* excision line (EcR^{99}/EcR^{M554fs}) at a stage comparable to around pupariation is indistinguishable from controls, showing an elaborate dendritic arbor with the characteristic branch (arrow). (E) CNS from a mutant (EcR^{99}/EcR^{M554fs}) at the stage of mouth hook detachment (see Fig. 4D). The SCP labeling pattern appears similar to the larval pattern with no sign of reduction (arrow), even though the CNS has undergone morphological changes indicating that development has progressed. (E) SCP labeling pattern in the *EcR-B1* specific mutant (EcR^{Q50st}/EcR^{M554fs}) at a stage comparable to around pupariation is characteristic of larval stages. (G) *EcR-B1* specific mutant CNS at the stage of mouth hook detachment shows a reduced dendritic arbor similar to the control at head eversion (C).

animals metamorphose reflects process regression and not loss of neuropeptide from neuronal processes.

In the *EcR-B* mutants the SCP pattern, at a stage corresponding to around pupariation, is indistinguishable from the control (Fig. 7D) with a dense mesh of dendrites in the anterior region of the ventral CNS. In the mutants that developed to the stage of mouth hook detachment (see Fig. 4D), a stage comparable to head eversion, the SCP pattern remains larval, despite the clear advancement of development of the CNS. Process regression did not occur and the dense dendritic arbors typical of younger stages are still present (Fig. 7E). The lack of pruning in older stage animals is consistent, and typical for all alleles tested (EcR^{214}, EcR^{225}, EcR^{31}, EcR^{80} and EcR^{99}), either in combination with an EcR null mutation or as homozygotes. These results indicated that the EcR-B isoforms have an essential role in the pruning back process during neuronal remodeling.

Since both EcR-B isoforms are eliminated in these mutants we can not ascribe pruning back to one or the other EcR-B isoform. Consequently, we also examined the SCP pattern in the *EcR-B1* specific mutant EcR^{W53st} (Bender et al., 1997). Most of these mutant larvae reach the third instar (Table 1) and have a phenotype similar to the late stage arrested animals of the *EcR-B* mutants described in this paper. Fig. 7F depicts the SCP projection pattern in a CNS from an *EcR-B1* animal (EcR^{W53st}/EcR^{M554fs}) at the time around pupariation, showing the characteristic arbors of the larval stage. At the time of mouth hook detachment (Fig. 7G) clear pruning back has taken place. In all CNS preparations examined we saw extensive process regression, though the degree was variable, with patterns similar to controls between 6 hours after pupariation and head eversion.

DISCUSSION

During metamorphosis of the CNS in *Drosophila*, distinct types of neuronal responses to ecdysteroids are correlated with expression of the EcR-A or EcR-B1 isoforms (Robinow et al., 1993; Truman et al., 1994). We have isolated *EcR* mutants that lack EcR-B1, and presumably also lack EcR-B2 expression, but retain EcR-A expression and used these mutants to examine EcR-B functions during larval neuron remodeling. Most *EcR-B* mutants arrest at the 1st and 2nd larval molts, demonstrating a requirement for EcR-B isoform functions during larval molting. Examination of *EcR-B* mutants that live to early metamorphosis shows that EcR-B isoforms are required for the early processes of larval remodeling in SCP-IR neurons of the CNS. Our observations provide evidence that remodeling of larval SCP-labeled neurons, like the remodeling of larval neurons in *Manduca*, is triggered by ecdysteroids and provide the first functional test of the model that different EcR isoforms control distinct cellular ecdysteroid responses in the CNS during metamorphosis (Robinow et al., 1993; Truman et al., 1994).

EcR-B isoforms are required for larval molting

The predominant time of death of *EcR-B* mutants is during the 1st and 2nd larval stages (Table 1). Many of the dead *EcR-B* mutants carry a duplicated larval cuticle (Fig. 4AB), suggesting that they have arrested during the process of larval molting. Interestingly, mutants that inactivate USP, which has been shown to be EcR's heterodimer partner by in vitro experiments (Koelle, 1992; Yao et al., 1992; Thomas et al., 1993), die at a similar time and also exhibit defects in larval molting (Perrimon et al., 1985; Oro et al., 1992). This similarity supports the hypothesis that EcR and USP also function together in vivo to mediate larval molting. Further evidence that the functional ecdysteroid receptor in vivo consists of EcR-USP heterodimers comes from analysis of *usp* mutants rescued beyond the early lethal phase by using a heat-shock driven usp^{+} transgene. These mutants arrest at the onset of metamorphosis and show defects strikingly similar to the late arrested EcR-B mutants (B. Hall and C.S. Thummel, personal communication).

The time of death of *EcR-B* mutants is in good accord with the time of EcR-B1 expression. Weak peaks of EcR-B1 mRNA and protein expression are detected in the second half of both the 1st and 2nd larval stages. Although EcR-A mRNA is not detected during the 1st or 2nd larval stages, low levels of EcR-A protein are detected during the 1st larval stage (Talbot et al., 1993). It is therefore possible that the somewhat heterogeneous time of death of *EcR-B* mutants is due to partial functional redundancy of the residual EcR-A protein. A similar heterogeneity in time of death has been reported for mutants in the ecdysteroid target genes E74A and E74B, which arrest development at several stages during metamorphosis (Fletcher et al., 1995).

EcR-B isoforms are required for metamorphosis of larval neurons

In experiments that use SCP immunoreactivity as a marker for cell morphology, we have shown that process regression of larval SCP-IR neurons is blocked in *EcR-B* mutants (Fig. 7E). We do not believe that this blockage is caused by a general arrest in development of the CNS as clear evidence of developmental progression of the CNS beyond the time of normal process regression is seen at both the morphological (Fig. 5A-C) and cellular (Fig. 5D-F) level. Changes in cellular morphology during metamorphosis including larval process regression and growth of adult processes have been well characterized in the SCP-IR neurons because the anatomy of these cells is reliably revealed using the SCP antibody (Truman, 1990). The SCP-IR neurons exhibit a type I pattern of EcR expression (Truman et al., 1994), characterized by high levels of EcR-B1 and low levels of EcR-A expression early in metamorphosis (Fig. 6), followed by a sharp drop in EcR-B1 expression and gradual increase in EcR-A expression such that EcR-A becomes the major isoform later in the pupal period. Thus, larval process regression in SCP-IR neurons is preceded by high level EcR-B1 expression while regrowth of adult-specific processes takes place at a time when EcR-A isoforms predominate. Although direct proof by ligation and hormone replacement experiments is lacking in *Drosophila*, blockage of process regression when the SCP-IR neurons lack EcR-B receptors suggests that neuronal remodeling in *Drosophila* is, like neuronal remodeling in *Manduca*, ecdysteroid induced. That this is generally true for neuronal remodeling in *Drosophila* is suggested by our preliminary data (M. S. and J. W. T., unpublished) that serotonergic neurons, a second set of identified larval neurons, also appear to fail to prune back their processes in *EcR-B* mutants.

Do different EcR isoforms govern distinct neuronal responses during metamorphosis?

The dynamic expression patterns of the EcR-A and EcR-B1 isoforms in the CNS and the correlation of specific EcR isoform expression with particular cellular responses are consistent with the hypothesis that EcR-A and EcR-B1 may each govern particular ecdysteroid responses in the CNS during metamorphosis (Robinow et al., 1993; Truman et al., 1994). Regression of larval processes of SCP-IR neurons, which express high levels of EcR-B1 and low levels of EcR-A prior to process regression, provided a well-defined system to test this hypothesis. Our finding that process regression is not blocked in *EcR-B1* mutants (Fig. 7G) is not consistent with the simplest form of this model. However, blockage of process regression is seen in *EcR-B* deletion mutants that lack EcR-B1 and presumably also lack EcR-B2 while retaining EcR-A expression (Fig. 7E). Below we consider three alternative hypotheses consistent with these data.

First, EcR-B1 and EcR-B2 may function redundantly to control larval process regression in SCP-IR neurons. In this model, removal of either EcR-B isoform would be insufficient to block larval neuron pruning; only removal of both isoforms would result in such blockage. This EcR regulatory mechanism would be distinct from that observed for other EcR-B1 predominant tissues at metamorphosis such as the larval and imaginal midgut and the larval salivary gland. In these tissues, loss of EcR-B1 resulted in failure of normal metamorphic responses (Bender et al., 1997). Possibly, EcR isoforms fulfill redundant functions in some developmental contexts, while in others they fulfill specific functions. An alternative hypothesis is that process regression is controlled solely by the EcR-B2 isoform. In this view, expression of the EcR-B1 isoform prior to the time of process regression in SCP-IR neurons would not be indicative of a role for this isoform in neuron remodeling. This model predicts that *EcR-B2* specific mutations, in contrast to *EcR-B1* specific mutations, would block larval process regression.

A third possibility is that the *EcR-B1* stop codon mutations are not complete null alleles and that residual EcR-B1 expression allows process regression in SCP-IR neurons. By western analysis, whole animal extracts of both stop codon mutants exhibit detectable levels of the 105 kDa wild-type EcR-B1 band (M. S. and J. W. T., T. Li and M. B., unpublished data). We estimate these levels to be <2% of wild-type (T. Li and M. B., unpublished data) and presume that the low levels of EcR-B1 protein detectable in these mutant extracts result from translational readthrough or ribosome hopping (Atkins et al., 1990). In this view, the effect of *EcR-B* mutations would be a consequence of removal of residual EcR-B1 protein rather than the EcR-B2 isoform. This model also necessitates that functional requirements for EcR-B1 levels be low in the SCP-IR neurons since we detect larval regression in these cells.

Definitive resolution of these alternative hypotheses will require the isolation of EcR-B2 specific mutants and/or determination of EcR-B2 expression in the CNS during metamorphosis. We do not know when or where EcR-B2 is expressed due to lack of an antibody directed against the 17 amino acid EcR-B2 specific N terminus and the absence of a probe specific to the EcR-B2 mRNA. Efforts are currently underway (T. Li and M. B.) to raise anti-peptide antibodies specific to the EcR-B2 specific domain to remedy this situation. Isolation of an *EcR-B2* mutant may be more difficult due to the small target size for mutagenesis and the fact that all *EcR-B2* exons are shared by the *EcR-B1* mRNA.

We currently favor the hypothesis that blockage of neuronal process regression in *EcR-B* but not *EcR-B1* mutants indicates functional redundancy of the EcR-B1 and EcR-B2 isoforms during dendritic pruning of SCP-IR neurons. Such apparent functional redundancy has been seen frequently in RAR knockout experiments in the mouse, with milder defects than expected if generated by loss of a single isoform (reviewed by Kastner et al., 1995; also discussed in Kastner et al., 1997). Recently, we have shown that activation of ecdysteroid target genes is defective in larval salivary gland cells of an *EcR-B1* mutant by assaying polytene chromosome puffing, and that this defect can be fully rescued by transgenic expression of EcR-B1 and partially rescued by expression of EcR-B2 (Bender et al., 1997). In contrast, EcR-A fails to rescue target gene activation in these cells. These results are consistent with the notion that EcR-B1 and EcR-B2 may be capable of functional substitution in certain cellular environments. Transient transfection experiments in an *EcR*$^{-}$ *Drosophila* cell line that show that EcR-B1 and EcR-B2 have similar transcriptional activation capabilities, distinct from that of EcR-A (X. Hu and P. Cherbas, personal communication), are also consistent with this model.

Regardless of the precise functional relationship between EcR-B isoforms, our results show that larval SCP-IR neurons require EcR-B isoform function to initiate dendritic pruning, and that the remaining levels of EcR-A cannot support this response. The question of whether EcR-A has distinct functions in neuronal maturation and cell death, as suggested by expression studies (Robinow et al., 1993; Truman et al., 1994), awaits genetic tests using EcR-A specific mutations. A more general question that remains is whether removal of EcR isoforms affects the endocrine system itself, given the strong expression of EcR-A and weaker expression of EcR-B1 in the ring gland (Talbot et al., 1993).

We thank J. Roote and M. Ashburner for providing the PW45-4 fly strain and M. Koelle and J. Willis for comments on the manuscript. UAS-tau flies were kindly provided by K. Ito. This work was supported by NIH grants GM53681 (to M. B.) and NS29971 (to J. W. T.), a grant from the University of Georgia Research Foundation (to M. B.), a National Research Service Award, GM07103, for pre-doctoral training in Genetics (to G. C.), and a Howard Hughes Summer Undergraduate Fellowship (to A. A. W.).

REFERENCES

Atkins, J. F., Weiss, R. B. and Gesteland, R. F. (1990). Ribosome gymnastics – degree of difficulty 9.5, style 10.0. *Cell* **62**, 413-423.

Bender, M., Imam, F. B., Talbot, W. S., Ganetzky, B. S. and Hogness, D. S. (1997). Drosophila ecdysone receptor mutations reveal functional differences among receptor isoforms. *Cell* **91**, 777-788.

Bier, E., Vaessin, H., Shepherd, S., Lee, K., McCall, K., Barbel, S., Ackerman, L., Carretta, R., Uemura, T., Grell, E., Jan, L. and Jan, Y. (1989). Searching for pattern and mutation in the *Drosophila* genome with a P-*lacZ* vector. *Genes Dev.* **3**, 1273-1287.

Brand, A. H. and Perrimon, N. (1993). Targeted gene expression as a means of altering cell fates and generating dominant phenotypes. *Development* **118**, 401-415.

Fletcher, J. C., Burtis, K. C., Hogness, D. S. and Thummel, C. S. (1995). The Drosophila E74 gene is required for metamorphosis and plays a role in

the polytene chromosome puffing response to ecdysone. *Development* **121**, 1455-1465.

Fristrom, D. and Fristrom, J. W. (1993). The metamorphic development of the adult epidermis. In *The Development of* Drosophila melanogaster, (ed. M. Bate and A. Martinez-Arias), pp. 843-898. Cold Spring Harbor: Cold Spring Harbor Laboratory Press,

Ito, K., Sass, H., Urban, J., Hofbauer, A. and Schneuly, S. (1997). Gal4-responsive UAS-tau as a tool for studying the anatomy and development of the Drosophila central nervous system. *Cell Tissue Res.* **290**, 1-10.

Jiang, C., Baehrecke, E. H. and Thummel, C. S. (1997). Steroid regulated programmed cell death during *Drosophila* metamorphosis. *Development* **124**, 4673-4683.

Kastner, P., Mark, M. and Chambon, P. (1995). Non-steroid nuclear receptors: What are genetic studies telling us about their role in real life? *Cell* **83**, 859-869.

Kastner, P., Mark, M., Ghyselinck, N., Krezel, W., Dupe, V., Grondona, J. M. and Chambon, P. (1997). Genetic evidence that the retinoid signal is transduced by heterodimeric RXR/RAR functional units during mouse development. *Development* **124**, 313-326.

Kimura, K. (1990). The regulatory gene of muscle cell death in Drosophila. *Saibokogaku* **9**, 55-61.

Koelle, M. R. (1992). *Molecular Analysis of the Drosophila Ecdysone Receptor Complex.* PhD Thesis, Stanford University, Stanford, CA.

Koelle, M. R., Talbot, W. S., Segraves, W. A., Bender, M. T., Cherbas, P. and Hogness, D. S. (1991). The Drosophila EcR gene encodes an ecdysone receptor, a new member of the steroid receptor superfamily. *Cell* **67**, 59-77.

Levine, R. B. and Weeks, J. C. (1996). Cell culture approaches to understanding the action of steroid hormones on the insect nervous system. *Dev. Neurosci.* **18**, 73-86.

Lundquist, T. and Nassel, D. R. (1990). Substance P-like, FMRFamide-like and gastrin/cholecystokinin-like immunoreactive neurons in the thoracico-abdominal ganglia of the flies Drosophila and Calliphora. *J. Comp. Neurol.* **294**, 161-178.

Masinovsky, B., Kempf, S. C., Callaway, J. C. and Willows, A. O. (1988). Monoclonal antibodies to the molluscan small cardioactive peptide SCPB: Immunolabeling of neurons in diverse invertebrates. *J. Comp. Neurol.* **273**, 500-512.

O'Hare, K. and Rubin, G. (1983). Structures of P transposable elements and their sites of insertion and excision in the *Drosophila melanogaster* genome. *Cell* **34**, 25-35.

Oro, A. E., McKeown, M. and Evans, R. M. (1992). The *Drosophila* retinoid X receptor homolog ultraspiracle functions in both female reproduction and eye morphogenesis. *Development* **115**, 449-462.

Perrimon, N., Engstrom, L. and Mahowald, A. P. (1985). Developmental genetics of the 2C-D region of the Drosophila X chromosome. *Genetics* **111**, 23-41.

Robertson, H. M., Preston, C. R., Phillis, R. W., Johnson-Schlitz, D. M., Benz, W. K. and Engels, W. R. (1988). A stable genomic source of P element transposase in Drosophila melanogaster. *Genetics* **118**, 461-470.

Robinow, S., Talbot, W. S., Hogness, D. S. and Truman, J. W. (1993). Programmed cell death in the *Drosophila* CNS is ecdysone-regulated and coupled with a specific ecdysone receptor isoform. *Development* **119**, 1251-1259.

Sambrook, J., Fritsch, E. F. and Maniatis, T. (1989). *Molecular Cloning: A Laboratory Manual*, Second Edition. Cold Spring Harbor: Cold Spring Harbor Laboratory Press.

Schneider, L. E., Sun, E. T., Garland, D. J. and Taghert, P. H. (1993). An immunocytochemical study of the FMRFamide neuropeptide gene products in Drosophila. *J. Comp. Neurol.* **337**, 446-460.

Taghert, P. H. and Schneider, L. E. (1990). Inter-specific comparison of a Drosophila gene encoding FMRFamide-related neuropeptides. *J. Neurosci.* **10**, 1929-1942.

Talbot, W. S., Swyryd, E. A. and Hogness, D. S. (1993). *Drosophila* tissues with different metamorphic responses to ecdysone express different ecdysone receptor isoforms. *Cell* **73**, 1323-1337.

Thomas, H. E., Stunnenberg, H. G. and Stewart, A. F. (1993). Heterodimerization of the Drosophila ecdysone receptor with retinoid X receptor and ultraspiracle. *Nature* **362**, 471-475.

Torok, T., Tick, G., Alvarado, M. and Kiss, I. (1993). *P-lacW* insertional mutagenesis on the second chromosome of *Drosophila melanogaster*: Isolation of lethals with different overgrowth phenotypes. *Genetics* **135**, 71-80.

Truman, J. W. (1990). Metamorphosis of the central nervous system in Drosophila. *J. Neurobiol.* **21**, 1072-1084.

Truman, J. W. (1996). Metamorphosis of the insect nervous system. In Metamorphosis: Postembryonic reprogramming of gene expression in amphibian and insect cells (ed. L. I. Gilbert, J. R. Tata and B. G. Atkinson), pp. 283-320. New York: Academic Press.

Truman, J. W., Talbot, W. S., Fahrbach, S. E. and Hogness, D. S. (1994). Ecdysone receptor expression in the CNS correlates with stage- specific responses to ecdysteroids during *Drosophila* and *Manduca* development. *Development* **120**, 219-234.

Truman, J. W., Taylor, B. J. and Awad, T. (1993). Formation of the adult nervous system. In *The Development of* Drosophila melanogaster (ed. M. Bate and A. Martinez-Arias), pp. 1245-1275. Cold Spring Harbor, New York: Cold Spring Harbor Laboratory Press.

Weeks, J. (1987). Time course of hormonal independence for developmental events in neurons and other cell types during insect metamorphosis. *Dev. Biol.* **124**, 163-176.

Weeks, J. C. and Truman, J. W. (1985). Independent steroid control of the fates of motoneurons and their muscles during insect metamorphosis. *J. Neurosci.* **5**, 2290-2300.

White, K., Hurteau, T. and Punsal, P. (1986). Neuropeptide-FMRFamide-like immunoreactivity in Drosophila: Development and distribution. *J. Comp. Neurol.* **247**, 430-438.

Yao, T.-P., Forman, B. M., Jlang, Z., Cherbas, L., Chen, J.-D., McKeown, M., Cherbas, P. and Evans, R. M. (1993). Functional ecdysone receptor is the product of *EcR* and *Ultraspiracle* genes. *Nature* **366**, 476-479.

Yao, T. P., Segraves, W. A., Oro, A. E., McKeown, M. and Evans, R. M. (1992). *Drosophila* ultraspiracle modulates ecdysone receptor function via heterodimer formation. *Cell* **71**, 63-72.

Yeo, S. L., Lloyd, A., Kozak, K., Dinh, A., Dick, T., Yang, X., Sakonju, S. and Chia, W. (1995). On the functional overlap between two Drosophila POU homeo domain genes and the cell fate specification of a CNS neural precursor. *Genes Dev.* **9**, 1223-1236.

Zipursky, S. L., Venkatesh, T. R., Teplow, D. B. and Benzer, S. (1984). Neuronal development in the Drosophila retina: monoclonal antibodies as molecular probes. *Cell* **36**, 15-26.